

# Preparation of thin electrolyte film via dry pressing/heating /quenching/ calcining for electrolyte-supported SOFCs



Hong Chang<sup>a</sup>, Jing Yan<sup>a</sup>, Huili Chen<sup>a,\*</sup>, Guangming Yang<sup>b</sup>, Jing Shi<sup>d</sup>, Wei Zhou<sup>b</sup>, Fangqin Cheng<sup>c</sup>, Si-Dian Li<sup>a</sup>, Zongping Shao<sup>b,e</sup>

<sup>a</sup> Institute of Molecular Science, Key Lab Mat Energy Convers & Storage Shanxi Province, Shanxi University, Taiyuan, 030006, PR China

<sup>b</sup> State Key Laboratory of Materials-Oriented Chemical Engineering, College of Chemistry & Chemical Engineering, Nanjing University of Technology, No. 5 Xin Mofan Road, Nanjing, 210009, PR China

<sup>c</sup> Institute of Resources and Environmental Engineering, Collaborative Innovation Center of High Value-added Utilization of Coal-related Wastes Shanxi University, Taiyuan, 030006, PR China

<sup>d</sup> Analytical Instrumentation Center, State Key Laboratory of Coal Conversion, Institute of Coal Chemistry, Chinese Academy of Sciences, 27 South Taoyuan Road, Taiyuan, 030001, PR China

<sup>e</sup> Department of Chemical Engineering, Curtin University, Perth, WA, 6845, Australia

## ARTICLE INFO

### Keywords:

Electrolyte-supported SOFCs  
Preparation method  
Thin electrolyte film  
Ni-YSZ

## ABSTRACT

The development of technologies used to prepare thin electrolyte films will stimulate the application of electrolyte-supported SOFCs since thin electrolyte films typically have low ohmic resistances and good electrochemical performance. This paper presents a novel method for the preparation of thin electrolyte films for yttria-stabilized zirconia (YSZ)-supported solid oxide fuel cells (SOFCs) via dry pressing/heating/quenching/calcining. The thicknesses of the as-prepared YSZ films were as low as 78 μm, which is significantly thinner than those prepared using a traditional method (greater than 200 μm) via dry pressing/calcining/polishing. More importantly, the preparation process was quicker. Using this novel method, a YSZ-supported cell with a configuration of (La<sub>0.6</sub>Sr<sub>0.4</sub>)<sub>0.9</sub>Co<sub>0.8</sub>Fe<sub>0.2</sub>O<sub>3-δ</sub> (LSCF)-Ce<sub>0.8</sub>Sm<sub>0.2</sub>O<sub>2-δ</sub>(SDC)/SDC/YSZ/SDC/Ba<sub>0.5</sub>Sr<sub>0.5</sub>Co<sub>0.8</sub>Fe<sub>0.2</sub>O<sub>3-δ</sub>(BSCF)-SDC was fabricated and tested. The results showed promising electrochemical performance and a peak power density of 0.64 W cm<sup>-2</sup> at 850 °C was obtained, which was much higher than the cell fabricated using the traditional method (0.29 W cm<sup>-2</sup>). The ohmic resistance ( $R_o$ ) at 850 °C is 0.19 Ω cm<sup>2</sup>, which is much lower than that of the cell fabricated using the traditional method (0.33 Ω cm<sup>2</sup>) at an identical temperature. The modified method described in this work is shown to be a promising technique to prepare thin electrolyte films for high-performance, electrolyte-supported SOFCs.

## 1. Introduction

A solid oxide fuel cell (SOFC) is a green energy conversion device that has a high efficiency (not limited by the Carnot cycle) and a low emission [1–7]. Classical SOFCs using yttria-stabilized zirconia (YSZ) as the electrolyte, have shown high performance and good reliability. However, YSZ has a low ion conductivity at low temperatures and works well only at temperatures higher than 850 °C, which causes several issues, such as longer start-up times and expensive specialized cell materials. Lowering the temperature of SOFC can offer a wider choice for cell components, reduce the start-up time, and improve the stability and efficiency of the cell [8–10]. One effective way to realize low-temperature SOFCs (LT-SOFCs) is to develop electrolyte materials with higher ionic conductivity at lower temperatures [11–14]. Cerium-

based electrolytes [15–20] and Mg- and Sr-doped LaGaO<sub>3</sub> (LSGM) [21–23] have been proposed as LT-SOFC electrolyte materials. However, for cerium-based electrolytes, Ce<sup>4+</sup> can be easily reduced to Ce<sup>3+</sup> under reducing conditions, which can cause internal short circuiting and cause n-type electronic conductivity [24,25]. On the other hand, LSGM poses several problems such as incompatibility with electrode materials, low mechanical strength, etc. [26–28]. Therefore, currently, zirconium-based electrolytes, such as YSZ, are considered to be the most stable and feasible electrolyte materials [29]. An alternative way to realize LT-SOFC is to reduce the thickness of the electrolyte layer [11–14]. Many papers have demonstrated that the performance of SOFCs is sensitive to the thickness of the electrolyte [30–32].

In an electrolyte-supported SOFC the YSZ electrolyte film is traditionally prepared via dry-pressing/calcining/polishing [29,33,34].

\* Corresponding author.

E-mail address: [huilichen@sxu.edu.cn](mailto:huilichen@sxu.edu.cn) (H. Chen).

<https://doi.org/10.1016/j.ceramint.2019.02.026>

Received 15 October 2018; Received in revised form 14 January 2019; Accepted 4 February 2019

Available online 05 February 2019

0272-8842/© 2019 Elsevier Ltd and Techna Group S.r.l. All rights reserved.

However, it is difficult to achieve a thin film with a thickness less than 200  $\mu\text{m}$  using this method. The thickness of the obtained pellet is usually too thick to be an electrolyte layer and it must be polished into a thinner one using sand paper. The polishing process is difficult to control, and it is time-consuming to obtain an even thickness due to the high mechanical strength after high-temperature calcination. Here, a modified method has been developed to prepare thin YSZ electrolyte films via dry-pressing/heating/quenching/calcining. This method was used to fabricate and test a YSZ-supported cell with a configuration of  $(\text{La}_{0.6}\text{Sr}_{0.4})_{0.9}\text{Co}_{0.8}\text{Fe}_{0.2}\text{O}_{3-\delta}$  (LSCF)– $\text{Ce}_{0.8}\text{Sm}_{0.2}\text{O}_{2-\delta}$  (SDC)/SDC/YSZ/SDC/ $\text{Ba}_{0.5}\text{Sr}_{0.5}\text{Co}_{0.8}\text{Fe}_{0.2}\text{O}_{3-\delta}$  (BSCF)–SDC. The cell was shown to exhibit excellent power output with a peak power density of  $0.64\text{ W cm}^{-2}$  at  $850\text{ }^\circ\text{C}$ , which is much higher than a cell prepared via a traditional method.

## 2. Experimental

### 2.1. Powder preparation

Nanoscale YSZ powder was provided by Shandong Jinao Technology Advanced Materials Co., Ltd.  $\text{Ce}_{0.8}\text{Sm}_{0.2}\text{O}_{2-\delta}$  (SDC) was synthesized by a hydrothermal method as follows:  $\text{Sm}(\text{NO}_3)_3 \cdot 6\text{H}_2\text{O}$  and  $\text{Ce}(\text{NO}_3)_3 \cdot 6\text{H}_2\text{O}$  were dissolved in ultrapure water with the mole ratio of  $\text{Ce}^{3+}:\text{Sm}^{3+}$  maintained at 4:1. Ammonia was added to the metal ion solution to adjust pH to 10, and then the solution was stirred and transferred to a Teflon-lined autoclave, and the sealed autoclave was heated at  $180\text{ }^\circ\text{C}$  for 24 h and quenched and cooled to room temperature using cold water. The products were filtered, washed with ethanol and ultrapure water several times, and then dried and sintered in a Muffle furnace at  $900\text{ }^\circ\text{C}$  for 5 h. This process is described in greater detail in a reported paper [35].

The anode material,  $(\text{La}_{0.6}\text{Sr}_{0.4})_{0.9}\text{Co}_{0.8}\text{Fe}_{0.2}\text{O}_{3-\delta}$  (LSCF), was synthesized by a conventional EDTA–CA complex process as reported. Briefly, stoichiometric amounts  $\text{Sr}(\text{NO}_3)_2$ ,  $\text{La}(\text{NO}_3)_3 \cdot 6\text{H}_2\text{O}$ ,  $\text{Fe}(\text{NO}_3)_3 \cdot 9\text{H}_2\text{O}$ , and  $\text{Co}(\text{NO}_3)_2 \cdot 6\text{H}_2\text{O}$  were dissolved in deionized water according to the molecular composition of  $(\text{La}_{0.6}\text{Sr}_{0.4})_{0.9}\text{Co}_{0.8}\text{Fe}_{0.2}\text{O}_{3-\delta}$ . Then, the coupling agents, CA and EDTA, were added to the solution at a molar ratio of CA:EDTA: $\text{M}^{n+}$  of 2:1:1. Ammonia was added to the solution to adjust the pH to 7. After stirring at  $90\text{ }^\circ\text{C}$ , solvent was slowly evaporated from the solution until a black gel formed. The gel was heated at  $260\text{ }^\circ\text{C}$  for 6 h and then calcined at  $950\text{ }^\circ\text{C}$  for 5 h in air.

The cathode material,  $\text{Ba}_{0.5}\text{Sr}_{0.5}\text{Co}_{0.8}\text{Fe}_{0.2}\text{O}_{3-\delta}$  (BSCF), was also prepared via the EDTA–CA process, and the obtained gel was fired at  $250\text{ }^\circ\text{C}$  and sintered at  $1100\text{ }^\circ\text{C}$  for 2 h.

### 2.2. Preparation of YSZ electrolyte films

In this work, two methods were used to fabricate the YSZ electrolytes: (a) a traditional method and (b) a modified method.

#### 2.2.1. Preparation of an electrolyte film via a traditional method

Firstly, a certain amount of YSZ powder (at least 0.1 g) was dry-pressed in a steel die to form a YSZ pellet with a 13 mm diameter. If the mass of the powder is less than 0.1 g, it is difficult to successfully form the pellet. Secondly, to obtain a dense pellet, the pellet was calcined at  $1400\text{ }^\circ\text{C}$  for 5 h. Finally, after cooling to room temperature, sandpaper was used to surface polish the pellet to obtain the desired thickness. It should be noted that after being calcined at  $1400\text{ }^\circ\text{C}$ , it was difficult to obtain a thin film with a thickness of less than 200  $\mu\text{m}$  by polishing due to the high mechanical strength of the YSZ pellet. In addition, it is believed that thinner electrolyte films are easier to be damaged when polishing with sandpaper. The YSZ pellet prepared via this traditional method is referred as YSZ-T.

#### 2.2.2. Preparation of an electrolyte film by a modified method

First, to obtain the support powder, a certain amount of PVB powder

and grass ash powder were thoroughly ground in a mortar at a mass ratio of 98:2. Then, the powder (0.06 g) was dry-pressed in a steel die to form a support layer. Afterwards 0.04 g of pure YSZ powder was rolled out homogeneously onto the support layer and uniaxially pressed to form a YSZ/support dual-layered pellet with a 13 mm diameter. Then, the pellet was heated in an oven at  $180\text{ }^\circ\text{C}$  for 1 h followed by liquid nitrogen treatment. The support layer was peeled off from the YSZ layer, covered by a small amount of YSZ powder, and the YSZ pellet was calcined at  $1400\text{ }^\circ\text{C}$  for 5 h. The YSZ pellet prepared by this modified method is labelled as YSZ-M and has a thickness of about 78  $\mu\text{m}$ .

### 2.3. Cell preparation

To prevent any side-reactions between the electrode materials and YSZ, an SDC electrolyte buffer layer was used. Specifically, the SDC powder was mixed uniformly with glycerol to obtain an SDC slurry, which was symmetrically sprayed on both surfaces of the YSZ electrolyte film with an air gun, and then subsequently sintered at  $1300\text{ }^\circ\text{C}$  for 5 h.  $(\text{La}_{0.6}\text{Sr}_{0.4})_{0.9}\text{Co}_{0.8}\text{Fe}_{0.2}\text{O}_{3-\delta}$  (LSCF)/SDC anode paste and  $\text{Ba}_{0.5}\text{Sr}_{0.5}\text{Co}_{0.8}\text{Fe}_{0.2}\text{O}_{3-\delta}$ /SDC cathode paste were sprayed onto the SDC buffer layer which had an active area of about  $0.278\text{ cm}^2$ . A diluted silver slurry was painted on the electrode surface as a current collector. Silver wires were attached to both the anode and the cathode to allow current to be conducted. Finally, a single cell with the structure of LSCF–SDC/SDC/YSZ/SDC/BSCF–SDC was attached to an alumina tube by silver paste, in which the anode side was oriented towards the inlet of the tube.

### 2.4. Characterization

The morphologies and microstructure of the samples were obtained using scanning electron microscopy (SEM, JSM-7001F, JEOL, Japan). The surface topographies of the YSZ films were examined using atomic force microscopy (AFM, Multimode 8, Bruker) in contact mode. The root-mean-square (RMS) roughness of the films was determined from the AFM images (Nanoscope Analysis 1.7). The electrochemical performances were performed using an Iviumstat electrochemical workstation with a four-probe configuration. During the I–V tests, hydrogen was fed into the anode chamber at a flow rate of  $80\text{ ml min}^{-1}$  (standard temperature and pressure), and the cathode was directly exposed to the ambient atmosphere. The I–V characteristics were recorded from  $750\text{ }^\circ\text{C}$  to  $850\text{ }^\circ\text{C}$  with a  $50\text{ }^\circ\text{C}$  interval. The EIS were also recorded under open circuit voltage (OCV) with an AC amplitude of 10 mV over a frequency range from 100 kHz to 0.1 Hz.

## 3. Results and discussion

### 3.1. A modified method for preparing thin YSZ electrolyte films

Fig. 1 shows the sequential steps used in the modified preparation method of a thin YSZ electrolyte film. A dual-layered pellet, composed of a support layer and a YSZ layer, was formed via step-by-step dry-pressing. Typically, the support layer is composed of colored organic substances, which can be easily removed by heating and quenching. In this work, the organic substances were PVB mixed with grass ash. To remove the support layer, the YSZ/support dual-layered pellet was heated in an oven at low temperatures to curl the PVB layer and cause it to delaminate from the YSZ layer. At this point, it was difficult to hold the PVB layer with a tweezer because the support layer was too viscous. When liquid nitrogen was used to quench the pellet, the support layer shrank and completely peeled off the YSZ electrolyte layer. Then, a small amount of YSZ powder was coated on the YSZ layer to prevent the YSZ pellet from twisting or cracking at high temperatures, which also helped achieve a reasonable flatness of the YSZ pellet.

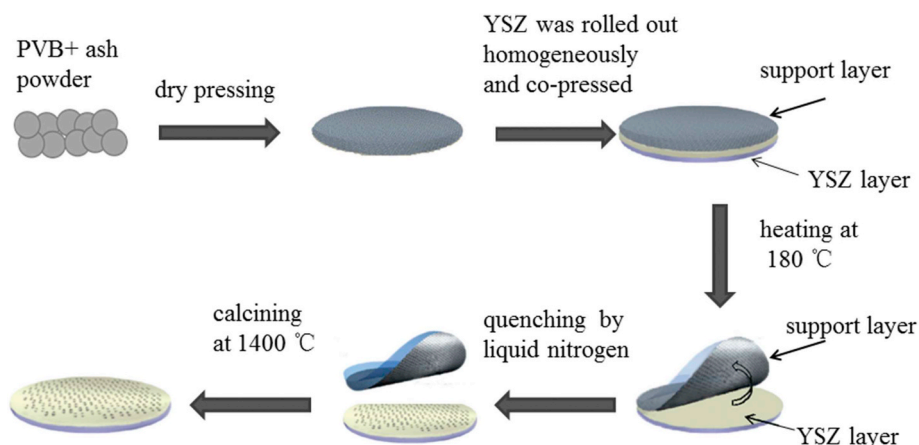


Fig. 1. The sequential steps for the preparation of the thin YSZ electrolyte film.

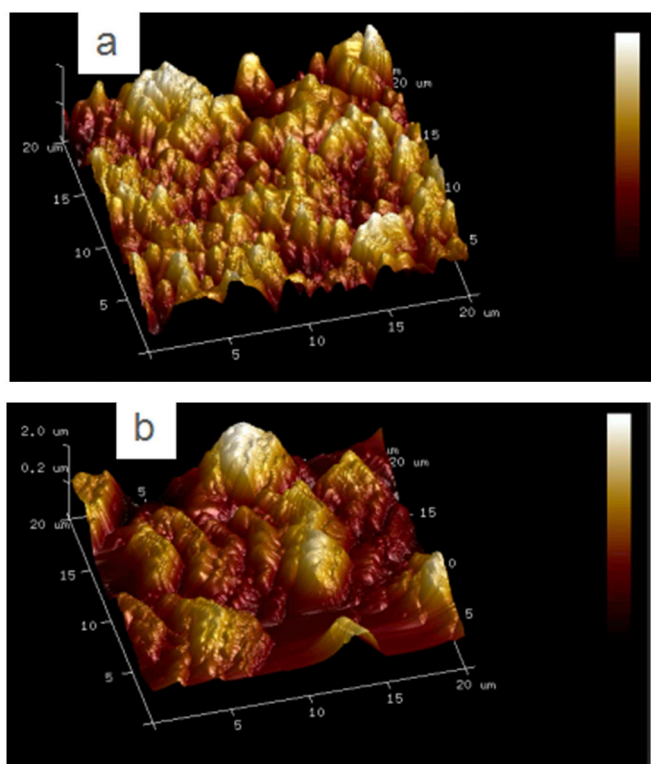


Fig. 2. AFM 3D height images of YSZ film that prepared by the traditional method (a), and by the modified method (b).

### 3.2. The surface topography and roughness of the YSZ films

Fig. 2 shows the surface topography and roughness of the YSZ films that were prepared using the traditional (YSZ-T) and the modified method (YSZ-M). The morphology of the YSZ-T exhibited hill-like structures with an RMS roughness of 226 nm (Fig. 2a), while YSZ-M exhibited dense hill-like structures with a higher RMS roughness of 493 nm (Fig. 2b). The above results indicate that YSZ-M had a very rough surface, so it was not necessary to roughen the surface with sandpaper. It is believed that the rough surface of the electrolyte is beneficial for close contact between the electrolyte and electrodes.

### 3.3. Microstructures of the cell

Two YSZ-supported cells with the LSCF–SDC/SDC/YSZ/SDC/BSCF–SDC structure were fabricated to include YSZ electrolyte films prepared by modified (YSZ-M, a) and traditional (YSZ-T, b) methods, respectively. Fig. 3 shows the cross-sectional microstructures of the two cells. For YSZ-M, a gas-tight electrolyte layer was obtained with a thickness around 78  $\mu\text{m}$ . Both the anode and cathode layers exhibited high porosity and close contact with the electrolyte layer (Fig. 3a). On the other hand, the thickness of the YSZ-T electrolyte layer was 230  $\mu\text{m}$ . It should be mentioned that some obvious delamination between the electrolyte and electrode layers was observed in Fig. 3b, which could be attributed to the smooth electrolyte surface due to uneven polishing. It is known that a rough surface is beneficial for the effective surface deposition of the electrode layer. The above results indicate that the modified method can be used to produce thinner YSZ electrolyte films with a rough surface compared to the traditional method.

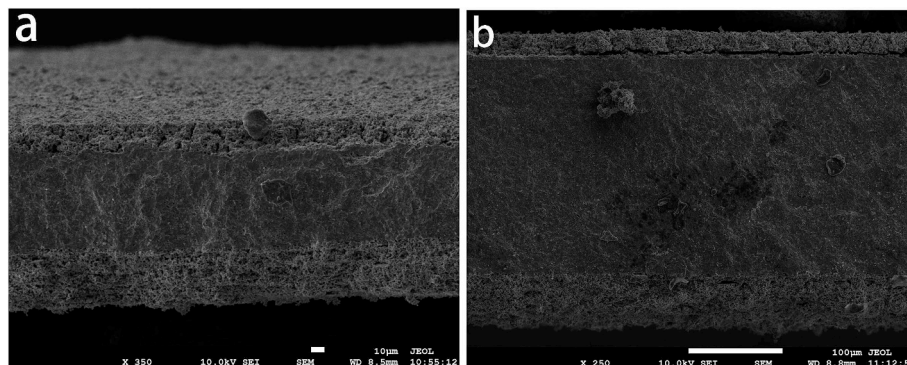


Fig. 3. The cross-sectional microstructures of the cells in which YSZ film was prepared using modified-(YSZ-M,a) and traditional (YSZ-T,b) method, respectively.

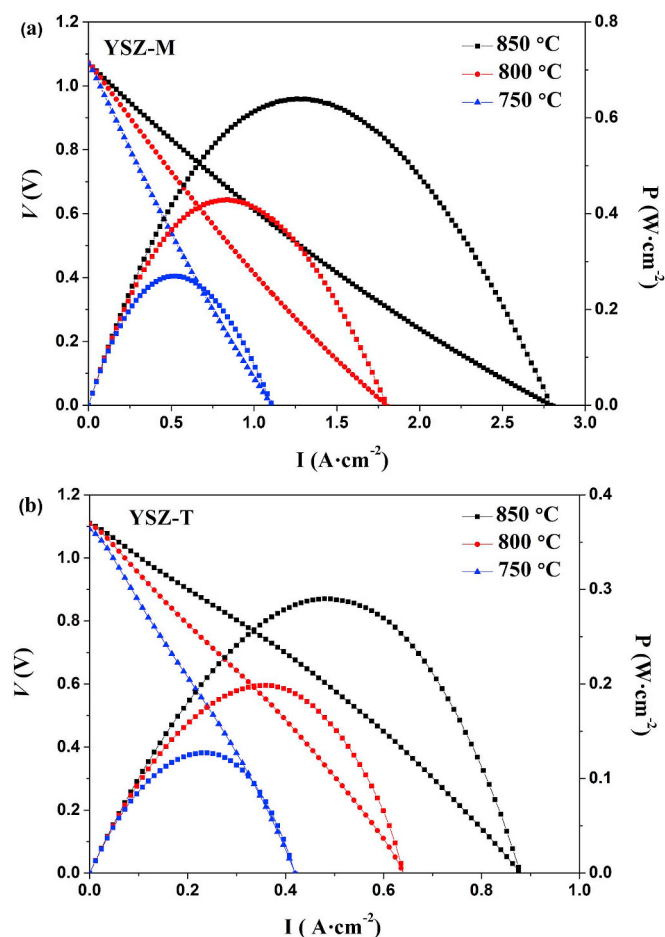


Fig. 4. I–V–P curves of the cells containing YSZ-M (a) and YSZ-T (b) when operating in an atmosphere of pure  $H_2$ .

### 3.4. Cell performance

Fig. 4 shows the cell performances (I–V–P) of the cells containing YSZ-T (thickness of YSZ around  $230 \mu\text{m}$ ) and YSZ-M (thickness of YSZ around  $78 \mu\text{m}$ ) when operating in an atmosphere of pure  $H_2$ . The open circuit voltages (OCVs) at  $850^\circ\text{C}$  were 1.109 and 1.068 V for YSZ-T and YSZ-M, respectively, which were close to the theoretical OCV value, indicating a dense electrolyte layer was formed. YSZ-T produced peak power densities (PPDs) of 0.29, 0.20, and  $0.13 \text{ W}\cdot\text{cm}^{-2}$  at 850, 800, and  $750^\circ\text{C}$ , respectively (Fig. 4a). In contrast, YSZ-M produced PPDs of 0.64, 0.43, and  $0.27 \text{ W}\cdot\text{cm}^{-2}$  (Fig. 4b) under identical conditions. Since the same cell materials and electrode fabrication methods were employed, it could be inferred that the difference in performance was mainly due to the thickness of the electrolyte layers. Fig. 5 a & b show a comparison of the electrochemical performances [I–V–P (a) and Nyquist plot of EIS (b)] between YSZ-T and YSZ-M at  $850^\circ\text{C}$  in dry  $H_2$ . YSZ-M showed much higher power and current outputs than YSZ-T (Fig. 5a). EIS was used to assess the electrochemical activity under the OCV conditions at  $850^\circ\text{C}$ . The Nyquist plots of the impedance spectra together with the simulated curves from the equivalent circuit of cells with YSZ-T and YSZ-M at  $850^\circ\text{C}$  in dry  $H_2$  are shown in Fig. 5b. The ohmic resistance ( $R_o$ ) is the high-frequency intercept with the real axis, which primarily correlates to the ionic resistance of the electrolyte [5,28,36]. Each resistance/constant phase element (R-CPE) couple can be assigned to a specific electrochemical process. The high-frequency resistance ( $R_H$ ) originates from the charge-transfer process at the interface of the electrode and electrode/electrolyte. The low-frequency resistance ( $R_L$ ) arises as a result of a mass-transfer process that includes gas-phase diffusion and dissociative adsorption [37]. Notably, the  $R_o$

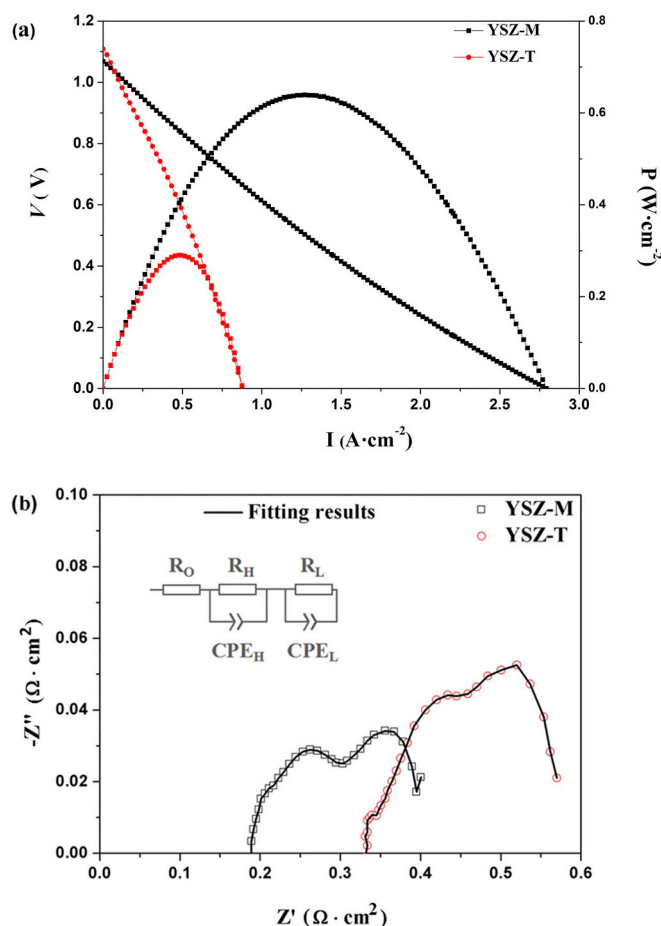


Fig. 5. The I–V (P) curves (a) and the Nyquist plot of EIS (b) of the cells containing YSZ-M (a) and YSZ-T (b) when operating in an atmosphere of pure  $H_2$ .

value of YSZ-M was  $0.19 \Omega \text{ cm}^2$ , which is much lower than that of YSZ-T ( $0.33 \Omega \text{ cm}^2$ ). The lower  $R_o$  of YSZ-M was attributed to the YSZ layer having a lower thickness. In addition, the  $R_H$  and  $R_L$  values of the cell with YSZ-T were  $0.44 \Omega \text{ cm}^2$  and  $0.51 \Omega \text{ cm}^2$ , respectively. While the  $R_H$  and  $R_L$  values of the cell fabricated with YSZ-M were reduced to  $0.43 \Omega \text{ cm}^2$  and  $0.38 \Omega \text{ cm}^2$ , respectively, under similar conditions. The decreased  $R_L$  is ascribed to the excellent contact between the electrolyte and electrodes due to the rough surface of the YSZ-M, which is beneficial to mass transfer. These results indicate that reducing the thickness of the electrolyte film could decrease the ohmic resistance, and the rough surface of the electrolyte film could hasten the mass transfer in an electrode process. Table 1 compares the data for some previously-reported YSZ-supported cells and the cell in this work in an  $H_2$  atmosphere. All the reported cells were fabricated via a traditional method with YSZ thicknesses from  $200 \mu\text{m}$  to  $400 \mu\text{m}$ , while the cell in this work had a thinner electrolyte layer and higher cell performance.

### 3.5. Advantages of the modified method for preparing thin YSZ electrolyte films

The above results demonstrate that this modified method via dry pressing/heating/quenching/calcining is an effective way to prepare a thin YSZ electrolyte film. Compared with the traditional method, the modified method has the following four advantages: (1) For an YSZ electrolyte pellet with a 13 mm diameter, the mass of YSZ powder could be reduced to 0.04 g, and a film as thin as  $78 \mu\text{m}$  could be obtained; (2) the thickness of the film can be controlled by the amount of YSZ powder; (3) after peeling from the PVB layer, the surface of the YSZ electrolyte layer was rough, and it was not necessary to further roughen

**Table 1**

Comparison of the data for some previously-reported YSZ-supported cells and the cell in this work in an H<sub>2</sub> atmosphere.

The structure of the cells	Thickness of the electrolyte (μm)	PPD (mW cm <sup>-2</sup> )	Temperature (°C)
LSTF SDC YSZ SDC LSTF [29]	400	374	900
		293	850
		205	800
LSCM YSZ LSCM [26]	200	300	900
		67.45	800
LSM YSZ LSM [28]	400	36.29	750
		18.34	700
		150.8	800
LSM-GDC YSZ  LSM-GDC[28]	400	87.84	750
		46.01	700
		639	850
This work	78	428	800
		270	750

the surface with sandpaper. Therefore, possible damage from the polishing process was fully avoided; (4) this modified method provided the electrolyte film with uniform thickness.

#### 4. Conclusions

Lowering the SOFC operating temperature to increase the life span of fuel cells and reduce cost is a major technical challenge. One approach to overcome this challenge is to reduce the electrolyte thickness. In this work, a modified dry-pressing method for preparing a dense and thin YSZ electrolyte film was developed. The results demonstrated that using a thin YSZ film improved the cell performance due to decreased ohmic resistance. This modified dry-pressing method offers a new possibility for preparing thin electrolyte films for electrolyte-supported SOFCs.

#### Acknowledgements

The authors gratefully acknowledge the financial support of this work by the Coal Seam Gas Joint Foundation of Shanxi (2015012016); Shanxi Province Science Foundation (2016011025); Shanxi Scholarship Council of China (2016-010); Shanxi “1331 Project” Key Innovative Research Team (1331KIRT) and Shanxi “1331 Project” Engineering Research Center (1331ERC). Thanks scientific instrument center of Shanxi University for the SEM test.

#### References

- Z. Shao, M.O. Tade, *Intermediate-Temperature Solid Oxide Fuel Cells*, Springer Berlin Heidelberg, 2016.
- H. Chang, H. Chen, Z. Shao, J. Shi, J. Bai, S.-D. Li, In situ fabrication of (Sr,La)FeO<sub>4</sub> with CoFe alloy nanoparticles as an independent catalyst layer for direct methane-based solid oxide fuel cells with a nickel cermet anode, *J. Mater. Chem.* 4 (36) (2016) 13997–14007.
- H. Chang, H. Chen, G. Yang, J. Shi, W. Zhou, J. Bai, Y. Wang, S.-D. Li, Enhanced coating resistance of Ni cermet anodes for solid oxide fuel cells based on methane on-cell reforming by a redox-stable double-perovskite Sr<sub>2</sub>MoFeO<sub>6-δ</sub>, *Int. J. Energy Res.* (2018), <https://doi.org/10.1002/er.4106>.
- L. Shao, Q. Wang, L. Fan, P. Wang, N. Zhang, K. Sun, Copper cobalt spinel as a high performance cathode for intermediate temperature solid oxide fuel cells, *Chem Commun (Camb)* 52 (55) (2016) 8615–8618.
- B. Ji, J. Wang, W. Chu, W. Yang, L. Lin, Acrylic acid and electric power cogeneration in an SOFC reactor, *Chem Commun (Camb)* 15 (2009) 2038–2040.
- D. Chen, C. Chen, Z.M. Baiyee, Z. Shao, F. Ciucci, Nonstoichiometric oxides as low-cost and highly-efficient oxygen reduction/evolution catalysts for low-temperature electrochemical devices, *Chem. Rev.* 115 (18) (2015) 9869–9921.
- N. Mahato, A. Banerjee, A. Gupta, S. Omar, K. Balani, Progress in material selection for solid oxide fuel cell technology: a review, *Prog. Mater. Sci.* 72 (2015) 141–337.
- N. Shaigan, W. Qu, D.G. Ivey, W.X. Chen, A review of recent progress in coatings, surface modifications and alloy developments for solid oxide fuel cell ferritic stainless steel interconnects, *J. Power Sources* 195 (6) (2010) 1529–1542.

- H.S. Noh, J.S. Park, J.W. Son, H. Lee, J.H. Lee, Physical and microstructural properties of NiO- and Ni-YSZ composite thin films fabricated by pulsed-laser deposition at T ≤ 700 °C, *J. Am. Ceram. Soc.* 92 (2009) 3059–3064.
- Z.P. Shao, S.M. Haile, J. Ahn, P.D. Ronney, Z. Zhan, S.A. Barnett, A thermally self-sustained micro solid-oxide fuel cell stack with high power density, *Nature* 435 (2005) 795–798.
- B. Shri Prakash, R. Pavitra, S. Senthil Kumar, S.T. Aruna, Electrolyte bi-layering strategy to improve the performance of an intermediate temperature solid oxide fuel cell: a review, *J. Power Sources* 381 (2018) 136–155.
- N. Pryds, K. Rodrigo, S. Linderoth, J. Schou, On the growth of gadolinia-doped ceria by pulsed laser deposition, *Appl. Surf. Sci.* 255 (2009) 5232–5235.
- C.C. Chao, C.M. Hsu, Y. Cui, F.B. Prinz, Improved solid oxide fuel cell performance with nanostructured electrolytes, *ACS Nano* 5 (7) (2011) 5692–5696.
- J.Y. Paek, I. Chang, J.H. Park, S. Ji, S.W. Cha, A study on properties of yttrium-stabilized zirconia thin films fabricated by different deposition techniques, *Renew. Energy* 65 (2014) 202–206.
- Y. Chen, J. Shen, G. Yang, W. Zhou, Z. Shao, A single-/double-perovskite composite with an overwhelming single-perovskite phase for the oxygen reduction reaction at intermediate temperatures, *J. Mater. Chem.* 5 (47) (2017) 24842–24849.
- M. Miyake, M. Iwami, M. Takeuchi, S. Nishimoto, Y. Kameshima, Electrochemical performance of Ni<sub>0.8</sub>Cu<sub>0.2</sub>/Ce<sub>0.8</sub>Gd<sub>0.2</sub>O<sub>1.9</sub> cermet anodes with functionally graded structures for intermediate-temperature solid oxide fuel cell fueled with syngas, *J. Power Sources* 390 (2018) 181–185.
- L.d. Santos-Gómez, J.M. Porras-Vázquez, E.R. Losilla, D. Marrero-López, Improving the efficiency of layered perovskite cathodes by microstructural optimization, *J. Mater. Chem.* 5 (17) (2017) 7896–7904.
- C. Yao, H. Zhang, X. Liu, J. Meng, X. Zhang, F. Meng, J. Meng, Investigation of layered perovskite NdBa<sub>0.5</sub>Sr<sub>0.25</sub>Ca<sub>0.25</sub>Co<sub>2</sub>O<sub>5+δ</sub> as cathode for solid oxide fuel cells, *Ceram. Int.* 44 (11) (2018) 12048–12054.
- J. Cao, Y. Ji, X. Huang, H. Jia, W. Liu, Tailoring the electron-blocking layer by addition of YSZ to Ba-containing anode for improvement of ceria-based solid oxide fuel cell, *Ceram. Int.* 44 (12) (2018) 13602–13608.
- J. Koettgen, S. Grieshammer, P. Hein, B.O.H. Grope, M. Nakayama, M. Martin, Understanding the ionic conductivity maximum in doped ceria: trapping and blocking, *Phys. Chem. Chem. Phys.* 20 (21) (2018) 14291–14321.
- L. Bian, C. Duan, L. Wang, R. O’Hayre, J. Cheng, K.C. Chou, Ce-doped La<sub>0.7</sub>Sr<sub>0.3</sub>F<sub>0.9</sub>Ni<sub>0.1</sub>O<sub>3-δ</sub> as symmetrical electrodes for high performance direct hydrocarbon solid oxide fuel cells, *J. Mater. Chem.* 5 (29) (2017) 15253–15259.
- J. Hwang, H. Lee, J.H. Lee, K.J. Yoon, H. Kim, J. Hong, J.-W. Son, Specific considerations for obtaining appropriate La<sub>1-x</sub>Sr<sub>x</sub>Ga<sub>1-y</sub>Mg<sub>y</sub>O<sub>3-δ</sub> thin films using pulsed-laser deposition and its influence on the performance of solid-oxide fuel cells, *J. Power Sources* 274 (2015) 41–47.
- C. Setevich, S. Larrondo, F. Prado, Infiltrated La<sub>0.5</sub>Ba<sub>0.5</sub>CoO<sub>3-δ</sub> in La<sub>0.8</sub>Sr<sub>0.2</sub>Ga<sub>0.8</sub>Mg<sub>0.2</sub>O<sub>2.8</sub> scaffolds as cathode material for IT-SOFC, *Ceram. Int.* 44 (14) (2018) 16851–16858.
- C. Neofytidis, V. Dracopoulos, S.G. Neophytides, D.K. Niakolas, Electrocatalytic performance and carbon tolerance of ternary Au-Mo-Ni/GDC SOFC anodes under CH<sub>4</sub>-rich Internal Steam Reforming conditions, *Catal. Today* 310 (2018) 157–165.
- P.C.C. Daza, R.A.M. Meneses, A.C.M. Rodrigues, C.R.M. da Silva, Ionic conductivities and high resolution microscopic evaluation of grain and grain boundaries of cerium-based codoped solid electrolytes, *Ceram. Int.* 44 (12) (2018) 13699–13705.
- L.S. Wang, C.X. Li, K. Ma, S.L. Zhang, G.J. Yang, C.J. Li, La<sub>0.8</sub>Sr<sub>0.2</sub>Ga<sub>0.8</sub>Mg<sub>0.2</sub>O<sub>3</sub> electrolytes prepared by vacuum cold spray under heated gas for improved performance of SOFCs, *Ceram. Int.* 44 (12) (2018) 13773–13781.
- L.S. Wang, C.X. Li, C.J. Li, G.J. Yang, Performance of La<sub>0.8</sub>Sr<sub>0.2</sub>Ga<sub>0.8</sub>Mg<sub>0.2</sub>O<sub>3</sub>-based SOFCs with atmospheric plasma sprayed La-doped CeO<sub>2</sub> buffer layer, *Electrochim. Acta* 275 (2018) 208–217.
- E.A. Filonova, A.R. Gilev, L.S. Skutina, A.I. Vylkov, D.K. Kuznetsov, V.Y. Shur, Double Sr<sub>2</sub>Ni<sub>1-x</sub>Mg<sub>x</sub>MoO<sub>6</sub> perovskites (x = 0, 0.25) as perspective anode materials for LaGaO<sub>3</sub>-based solid oxide fuel cells, *Solid State Ionics* 314 (2018) 112–118.
- D.M. Bastidas, S. Tao, J.T.S. Irvine, A symmetrical solid oxide fuel cell demonstrating redox stable perovskite electrodes, *J. Mater. Chem.* 16 (17) (2006) 1603.
- B. Singh, S. Ghosh, S. Aich, B. Roy, Low temperature solid oxide electrolytes (LT-SOE): a review, *J. Power Sources* 339 (2017) 103–135.
- D.H. Myung, J. Hong, K. Yoon, B.K. Kim, H.W. Lee, J.H. Lee, J.W. Son, The effect of an ultra-thin zirconia blocking layer on the performance of a 1-μm-thick gadolinia-doped ceria electrolyte solid-oxide fuel cell, *J. Power Sources* 206 (2012) 91–96.
- P.C. Su, C.C. Chao, J.H. Shim, R. Fasching, F.B. Prinz, Solid oxide fuel cell with corrugated thin film electrolyte, *Nano Lett.* 8 (8) (2008) 2289–2292.
- X. Luo, Y. Yang, Y. Yang, D. Tian, X. Lu, Y. Chen, Q. Huang, B. Lin, Reduced-temperature redox-stable LSM as a novel symmetrical electrode material for SOFCs, *Electrochim. Acta* 260 (2018) 121–128.
- Z. Cao, Y. Zhang, J. Miao, Z. Wang, Z. Lü, Y. Sui, X. Huang, W. Jiang, Titanium-substituted lanthanum strontium ferrite as a novel electrode material for symmetrical solid oxide fuel cell, *Int. J. Hydrogen Energy* 40 (6) (2015) 16572–16577.
- H.G. Shi, W. Zhou, R. Ran, Z.P. Shao, Comparative study of doped ceria thin-film electrolytes prepared by wet powder spraying with powder synthesized via two techniques, *J. Power Sources* 195 (2) (2010) 393–401.
- G.D. Han, H.J. Choi, K. Bae, H.R. Choi, D.Y. Jang, J.H. Shim, Fabrication of lanthanum strontium cobalt ferrite-gadolinium-doped ceria composite cathodes using a low-price inkjet printer, *ACS Appl. Mater. Interfaces* 9 (45) (2017) 39347–39356.
- Z.G. Lu, J.H. Zhu, Z.H. Bi, X.C. Lu, A Co-Fe alloy as alternative anode for solid oxide fuel cell, *J. Power Sources* 180 (1) (2008) 172–175.